

LA-UR- 09-03610

Approved for public release;  
distribution is unlimited.

Title:	Overview of the Proton Radiography Facility at LANSCE
Author(s):	Fesseha G. Mariam
Intended for:	Weapons Agency Nondestructive Testing Organization 44th WANTO Meeting



Los Alamos National Laboratory, an affirmative action/equal opportunity employer, is operated by the Los Alamos National Security, LLC for the National Nuclear Security Administration of the U.S. Department of Energy under contract DE-AC52-06NA25396. By acceptance of this article, the publisher recognizes that the U.S. Government retains a nonexclusive, royalty-free license to publish or reproduce the published form of this contribution, or to allow others to do so, for U.S. Government purposes. Los Alamos National Laboratory requests that the publisher identify this article as work performed under the auspices of the U.S. Department of Energy. Los Alamos National Laboratory strongly supports academic freedom and a researcher's right to publish; as an institution, however, the Laboratory does not endorse the viewpoint of a publication or guarantee its technical correctness.

## Overview of the Proton radiography Facility at LANSCE

### Abstract:

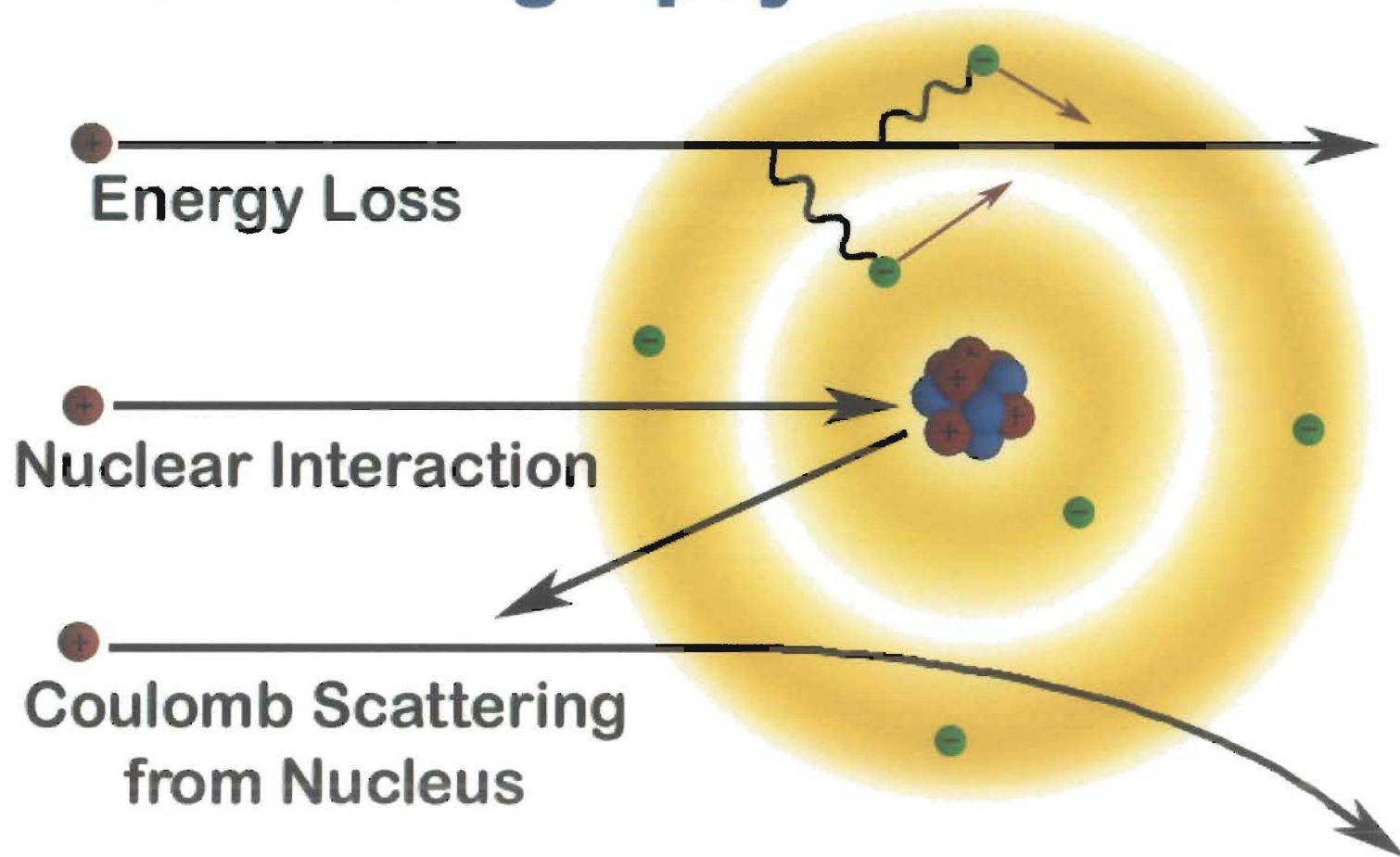
The Proton Radiography Facility at LANSCE, has been a useful tool for studying dynamic processes on time scales of fractions of a microsecond and with resolutions of a few tenths of mm to a few tenths of a micrometer . This overview is an expose of the this radiography system - its operating principles and capabilities and limitations.

# Overview of the Proton Radiography Facility at LANSCE

Fesseha G. Mariam  
(for the PRAD Team)

# Proton Interactions

## Proton Radiography



# Early Proton Radiography

A. M. Koehler, *et al.* *Science* 160, 303 (1968)



Fig. 1. Proton radiograph of aluminum absorber 7 cm in diameter and 18 g/cm<sup>2</sup> thick, with an additional thickness of 0.03 g/cm<sup>2</sup> aluminum foil, cut in the shape of a paintbrush, inserted at a depth of 9 g/cm<sup>2</sup>. The addition of 0.2 percent to the total thickness produces a substantially darker area on the film.

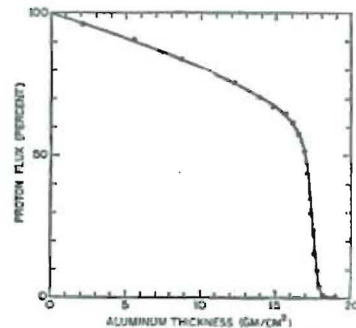


Fig. 2. Proton flux as a function of depth in aluminum. The steeply falling portion of the curve near 18 g/cm<sup>2</sup> is used to obtain the high contrast of Fig. 1.

J. A. Cookson *Naturwissenschaften* 61, 184—191 (1974)

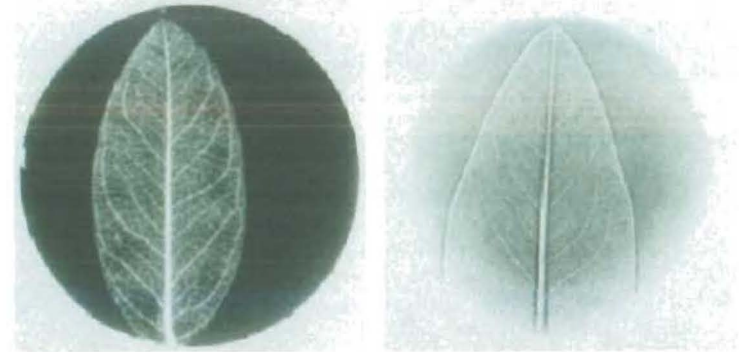


Fig. 6a and b. Radiographs of leaves by a) marginal range radiography with 196 mg/cm<sup>2</sup> of extra Al absorber, and b) scattering radiography with leaf sandwiched between two 6.9 mg/cm<sup>2</sup> Al layers and 14 mm from the film

## Marginal Range Radiography

- Reduce proton beam energy to near end of range.
- Use steep portion of transmission curve to enhance sensitivity to areal density variations.
- Coulomb scattering at low energy results in poor resolution >1.5 mm.
- Contrast generated through proton absorption.

## Scattering Radiography

- Edge detection only
- Limited to thin objects
- Contrast generated through position dependent scattering

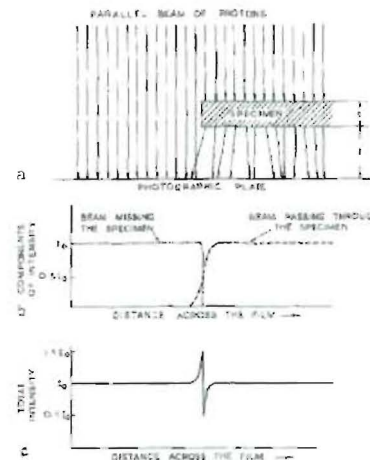
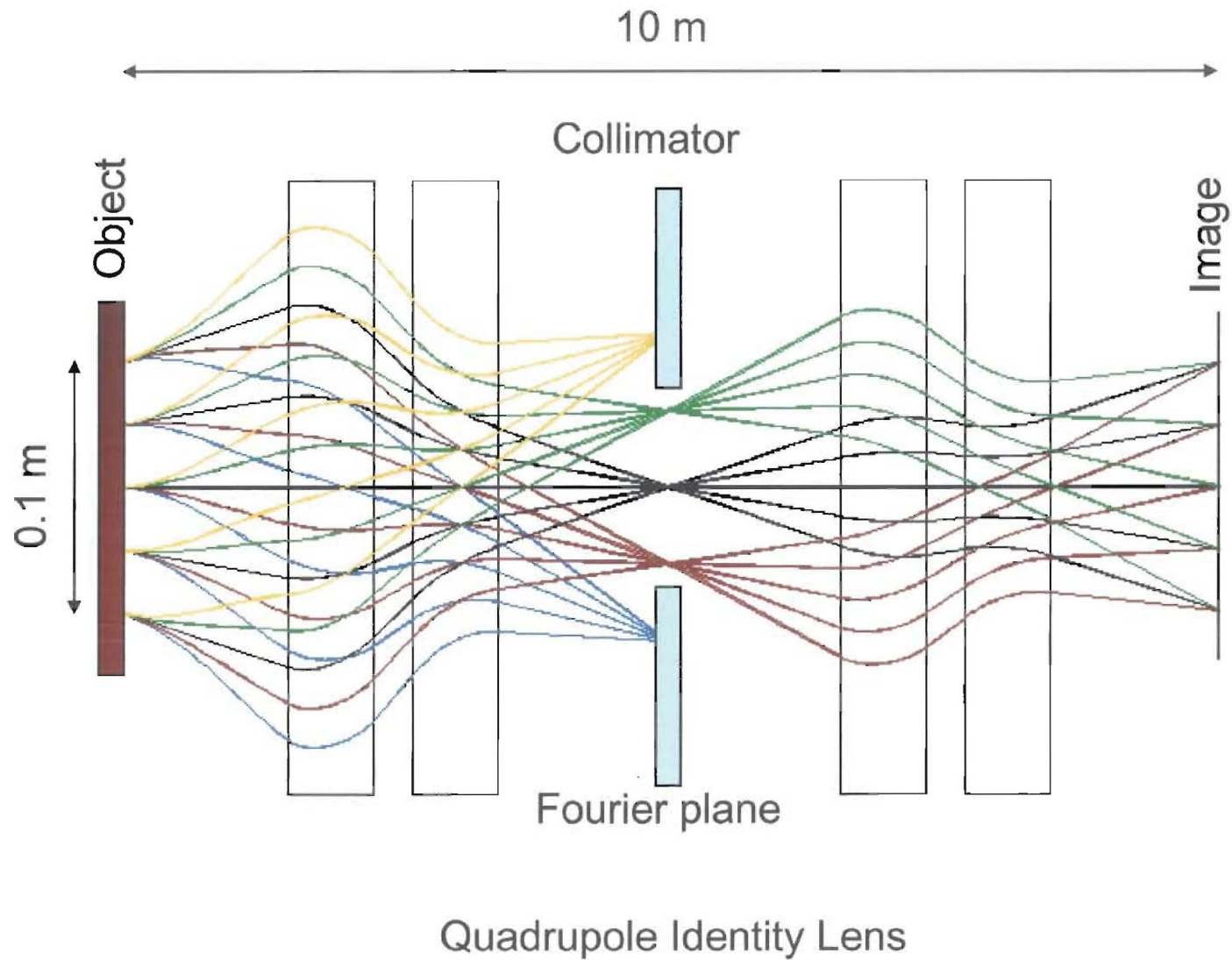
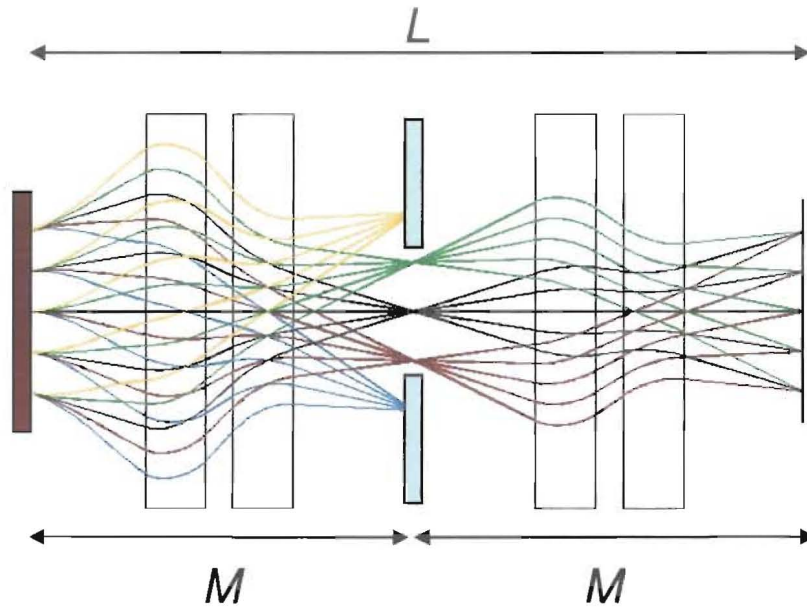


Fig. 7. Illustration of how multiple scattering produces its characteristic edge pattern

# Magnetic Imaging Lens



# Matching Miracle



- $x_o, x_o'$  - position and angle at object
- $x_{fp}$  - position at midpoint of lens
- $x_i$  - position and angle at image
- $\delta$  -  $\Delta p/p$
- $M$  - Transport matrix for doublet
- $L$  - First order Transport matrix
- $T$  - Second order Transport tensor

$$L = M^2 = -I$$

## Fourier Plane

$$x_{fp} = M_{11}x_o + M_{12}x_o'$$

$$x_o' = wx_o + \phi$$

$$x_{fp} = M_{11}x_o + M_{12}(wx_o + \phi)$$

$$w = \frac{-M_{11}}{M_{12}}$$

$$x_{fp} = M_{12}\phi$$

Form identity lens from identical doublets

Inject beam with position-angle correlation to form Fourier plane at center of lens.

## Resolution

$$x_i = L_{11}x_o + L_{12}x_o' + T_{116}x_o\delta + T_{126}x_o'\delta$$

$$x_i = -x_o + T_{116}x_o\delta + T_{126}(wx_o + \phi)\delta$$

$$w = \frac{-T_{116}}{T_{126}} = \frac{-M_{11}}{M_{12}} \quad *$$

$$w = \frac{-M_{11}}{M_{12}}$$

$$\Delta x_i = T_{126}\phi\delta$$

Dominant Blur

Same position-angle correlation cancels second order chromatic terms.

\* C.T. Mottershead and J. D. Zumbro, "Magnetic Optics for Proton Radiography", Proceedings of the 1997 Particle Accelerator Conference

# Areal Density Reconstruction

$$T_{nuclear} = e^{-x/\lambda}$$

Nuclear removal processes

---

$$T_{MCS} = 1 - e^{-\theta_c^2 / 2\theta_o^2}$$

$$\theta_o = \frac{14.1 \text{ MeV}}{p\beta} \sqrt{\frac{x}{x_o}}$$

Multiple Coulomb Scattering with collimation:

☺<sub>o</sub> - scattering angle (radians)

$x$  - areal density

$x_o$  - radiation length

$p$  - momentum (MeV)

$\beta$  - relativistic velocity

---

$$T = e^{-x/\lambda} \left( 1 - e^{-\left(\frac{\theta_c p \beta}{14.1 \text{ MeV}}\right)^2 \frac{x_o}{2x}} \right)$$

Total Transmission

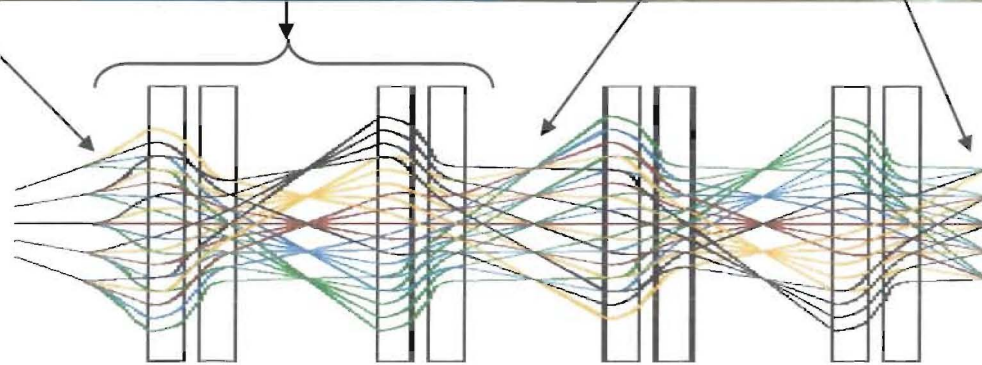
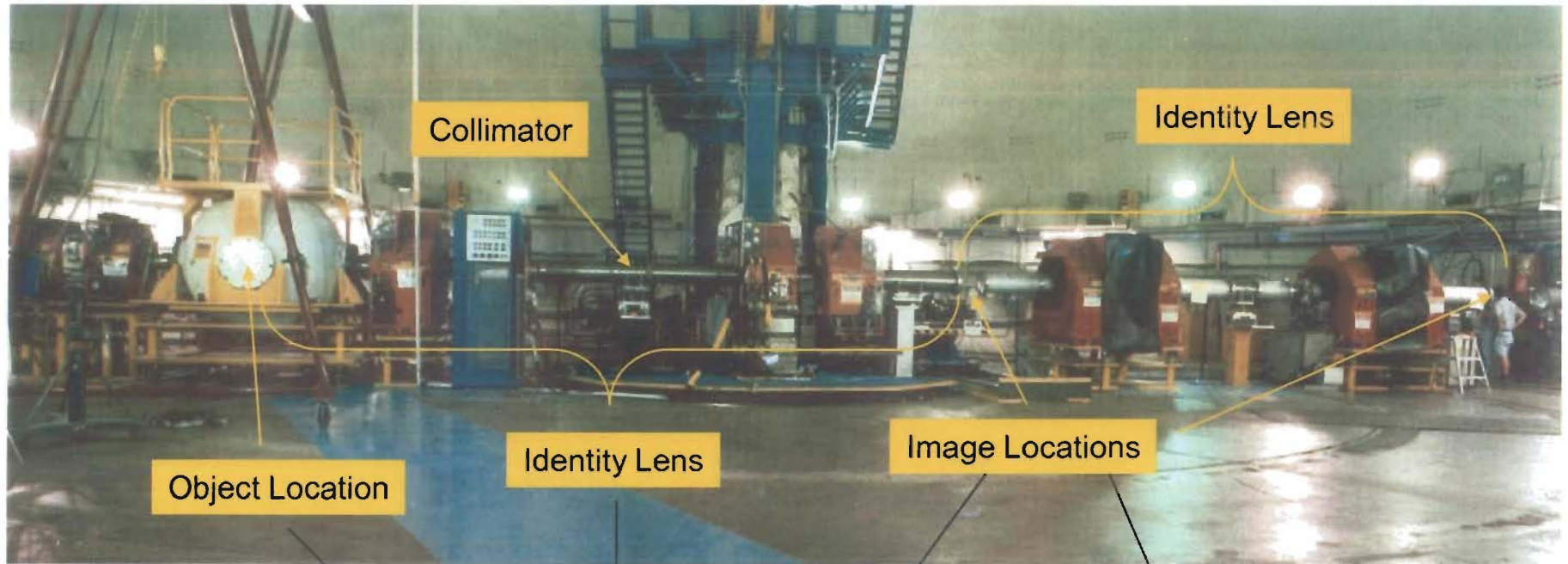
- inverted to determine areal density,  $x$

# LANSCCE Experimental Areas



- Lujan Center
  - *National security research*
  - *Materials, bio-science, and nuclear physics*
  - *National user facility*
- WNR
  - *National security research*
  - *Nuclear Physics*
  - *Neutron Irradiation*
- Proton Radiography
  - *National security research*
  - *Dynamic Materials science,*
  - *Hydrodynamics*
- Isotope Production Facility
  - *Medical radioisotopes*

# pRad Facility at LANSCE



# x3 Magnifier



Lens made up of four 4" bore permanent magnet quads.

Tuning (focusing) is done by remotely moving quads in some prescribed manner

System has approximately 3 times less chromatic aberration than -I (big) lens

Price is: FOV is three times less than that with the -I lens

For magnifier operations, Lens2 is off

# x7 Magnifier

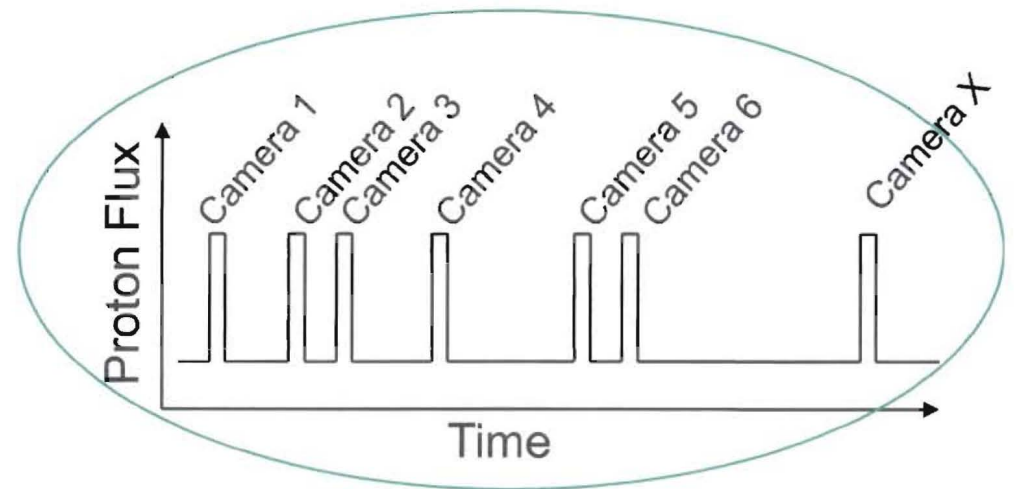
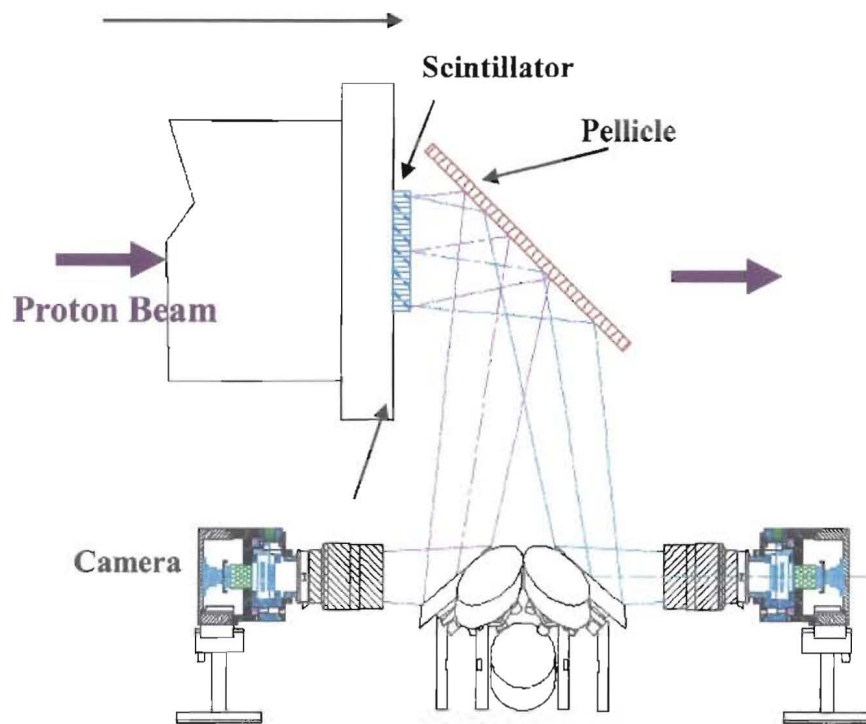
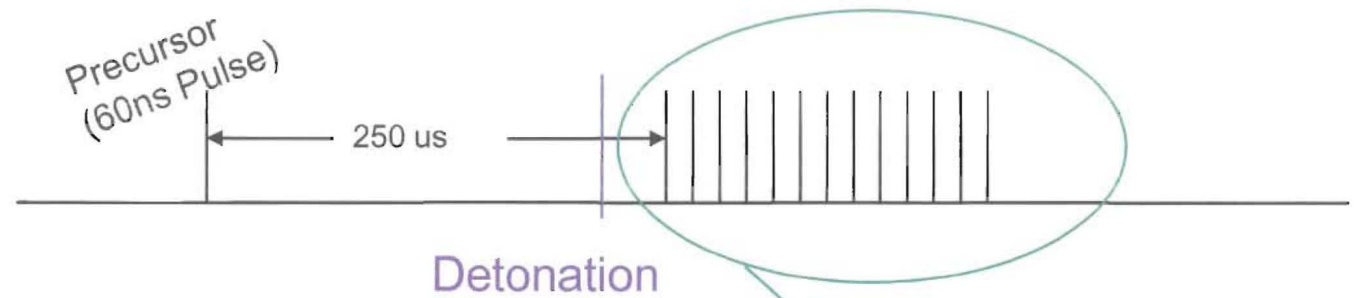


Similar to the x3 magnifier.

Made up of four 1" bore permanent magnet quads.

Yet has to be commissioned properly

# Camera System and Standard Timing

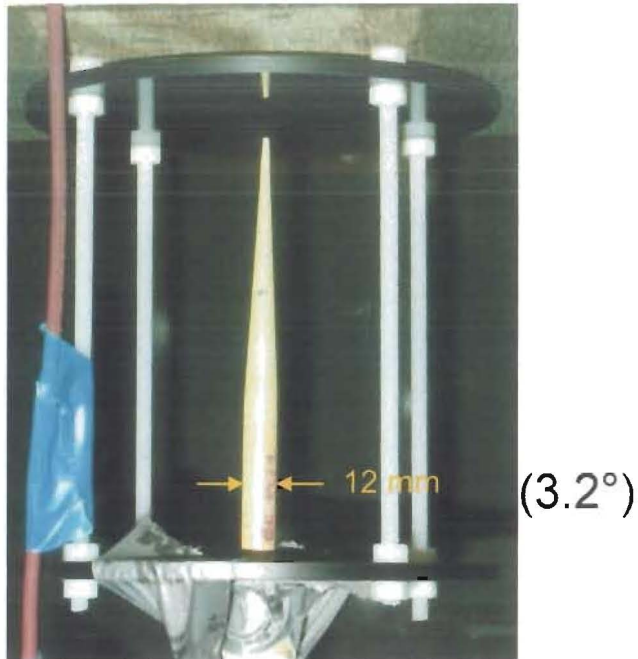


- 19 images at first station (IL1)
- 22 images at second station (IL2)
- Typically 50 to 200 ns exposure times

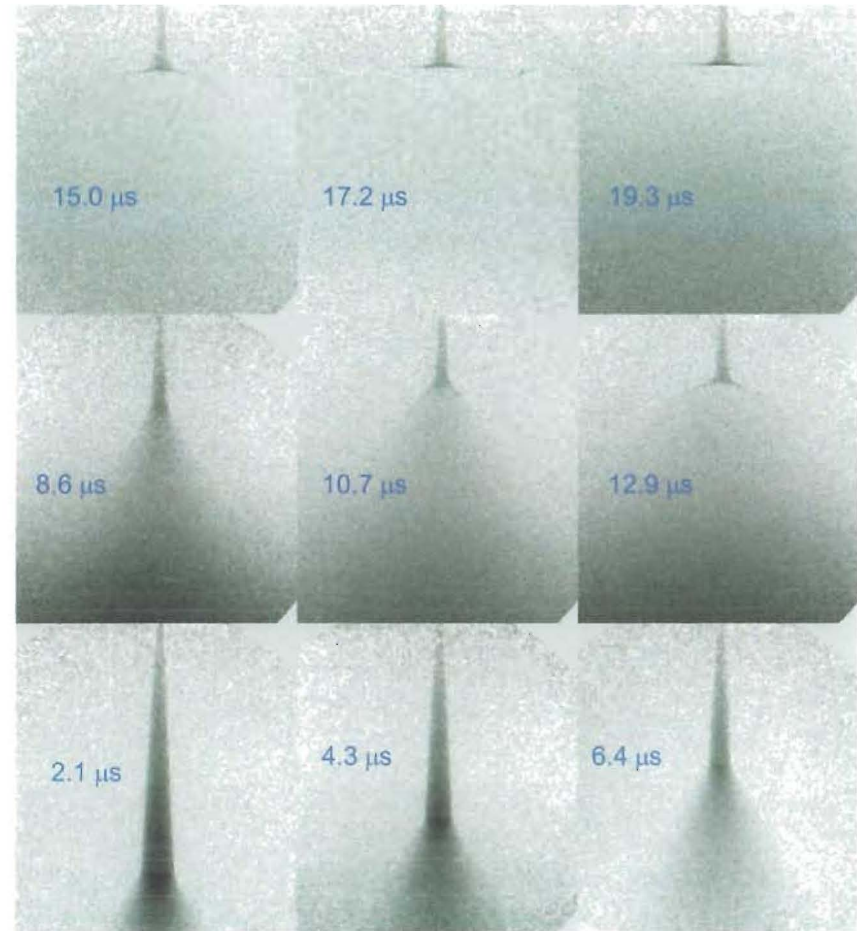
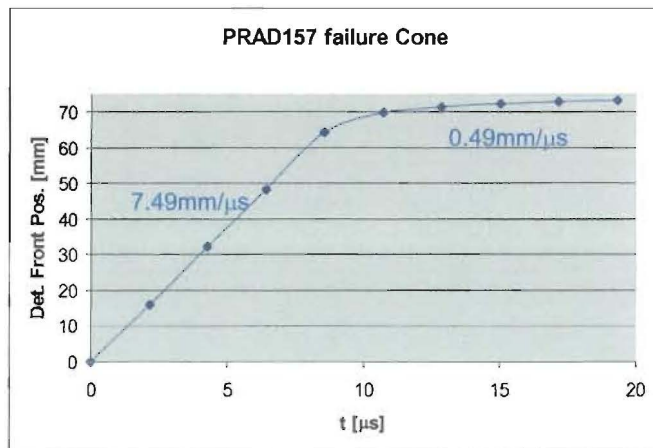
# The camera Table at IL1



# Failure Cone (Eric Ferm)



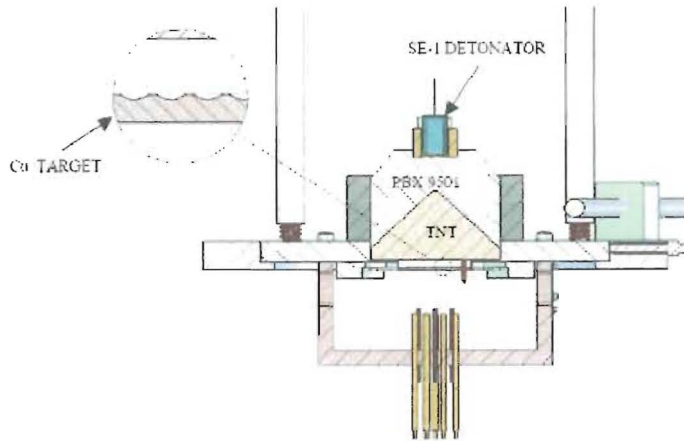
Failure occurs at  $d=5.4$  to  $5.6$ mm



# 25 mm cone, (7.1°)

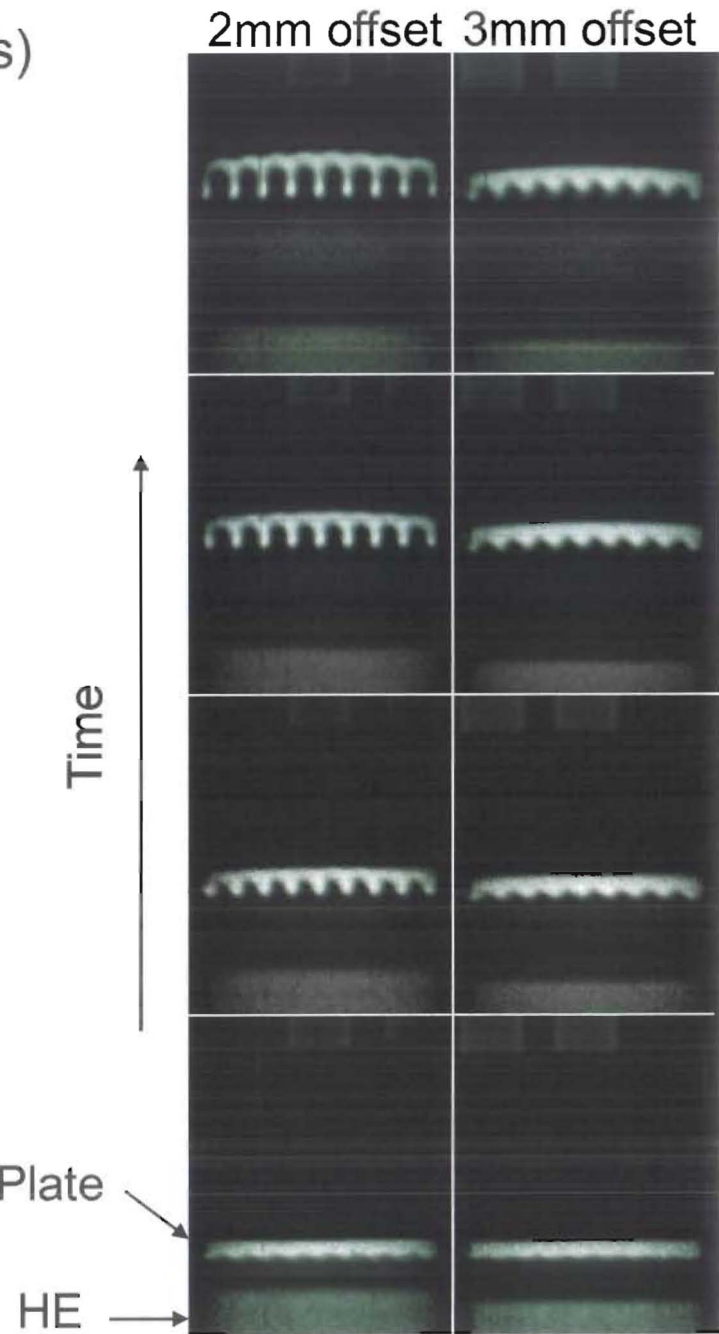


# Material Strength Experiments (Olson Series)

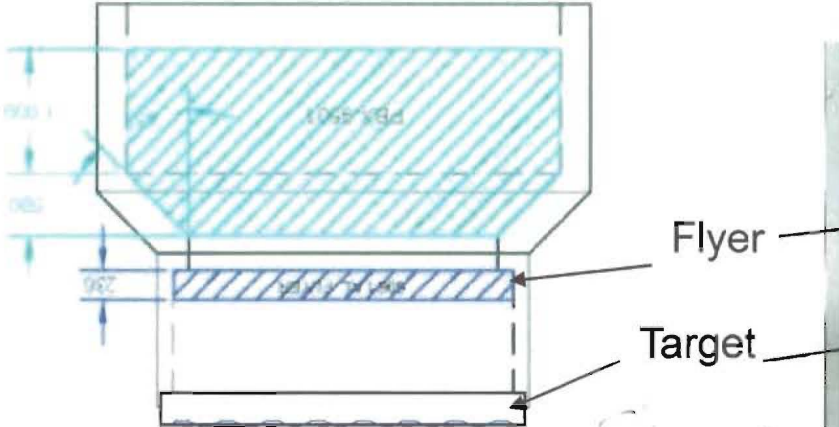


The technique utilizes a flat metal plate with perturbations of known wavelength and amplitude machined into one side of the plate. High explosive is used to generate shock-free, planar loading on the perturbed side of the plate and the amplitude of the Rayleigh-Taylor (R-T) unstable perturbations are measured from radiographs acquired as a function of time. The perturbation growth rate is directly related to the dynamic shear strength of the metal and thus can be compared directly to that predicted by various strength models via hydrodynamic calculations.

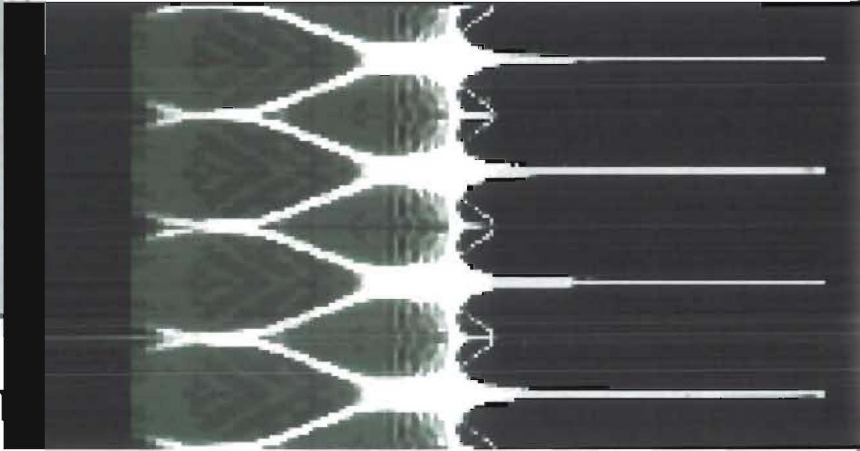
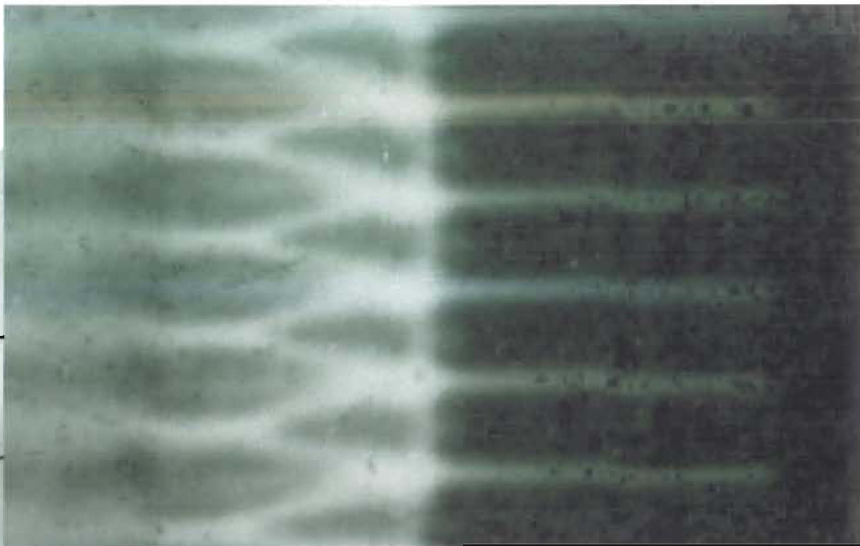
- Utilized improved resolution capability of new magnifier system.
- Six dynamic experiments performed to study instability growth versus drive pressure by varying HE standoff.
- Demonstrated shockless acceleration and reproducibility.



pRad has been used to make a movie of the development of a Richtmyer-Meshkov (RM) instability in molten tin (W. Buttler)



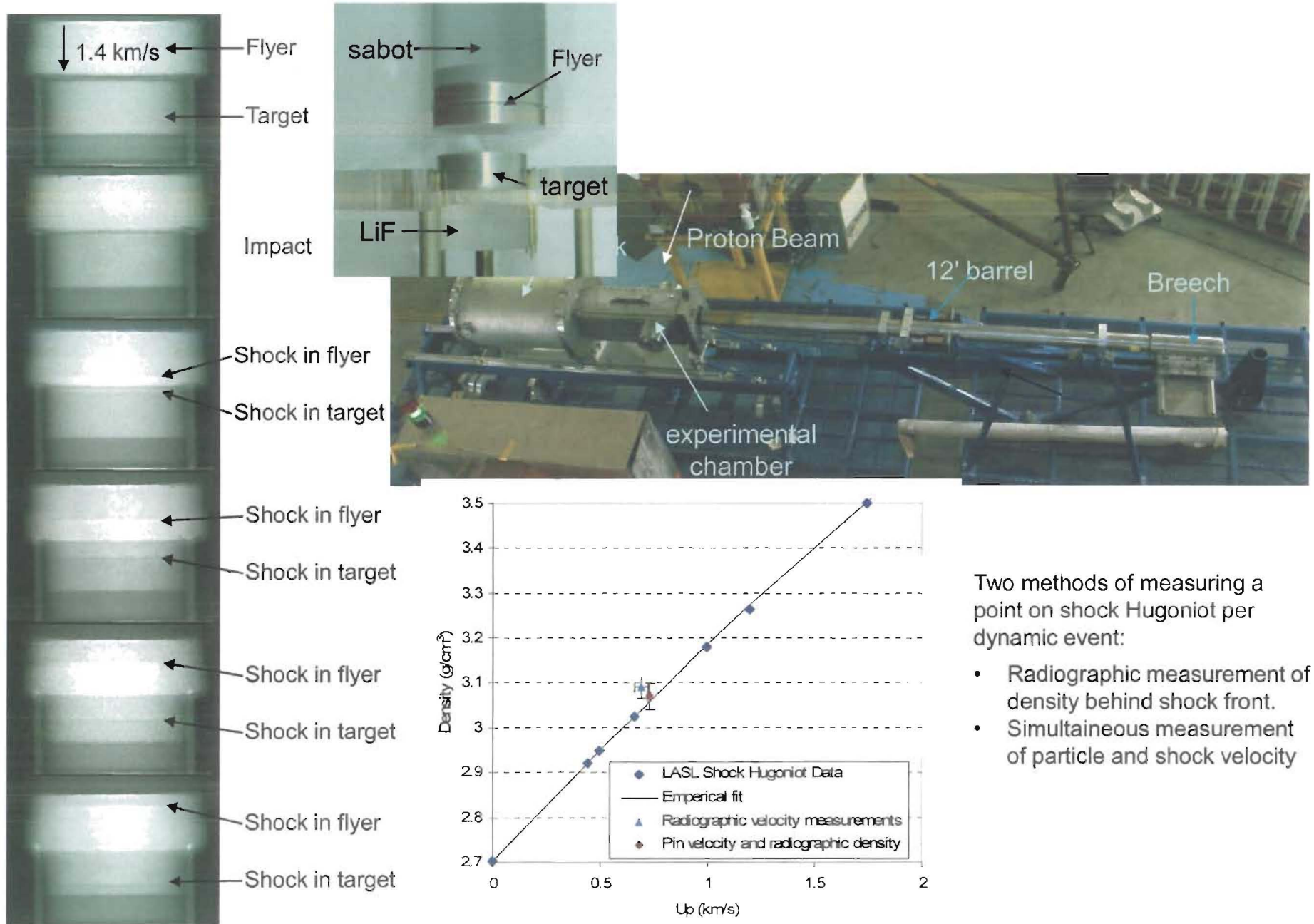
Show movie



er face

Hydrodynamic Calculations (David Youngs et al.)

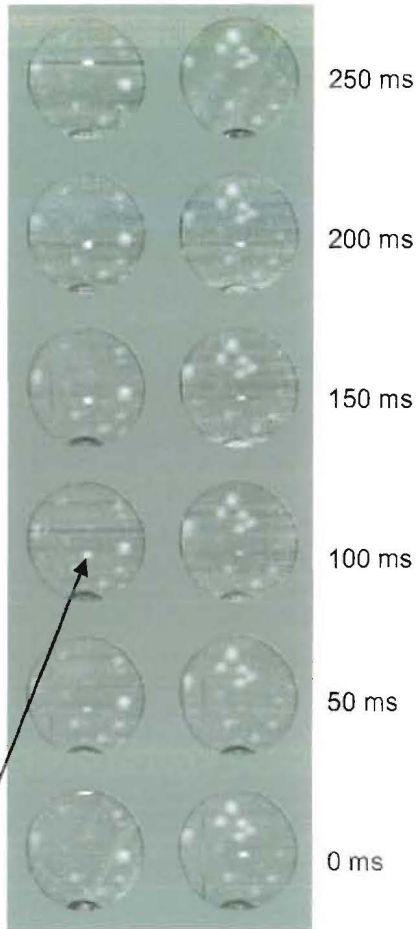
# Demonstration of new EOS measurement capability with proton Radiography



Two methods of measuring a point on shock Hugoniot per dynamic event:

- Radiographic measurement of density behind shock front.
- Simultaneous measurement of particle and shock velocity

# Quasi Static Systems (msec to seconds): Dynamic studies of He Bubble formation in Hg in Support of the SNS High Current Target Development



Bubbler Needle Tip

He bubble formation in stagnant (left) and flowing (right) mercury.

In the case of the stagnant Hg, the bubbles form, grow in size and break off in about  $\frac{1}{4}$  sec. When the Hg is flowing, the bubbles break off at much faster time scales.

Thousands of such pictures were taken with the Rockwell cameras in movie mode at 20Hz under various He and Hg flow rates.

# Static Objects Surrogate Fuel Rods



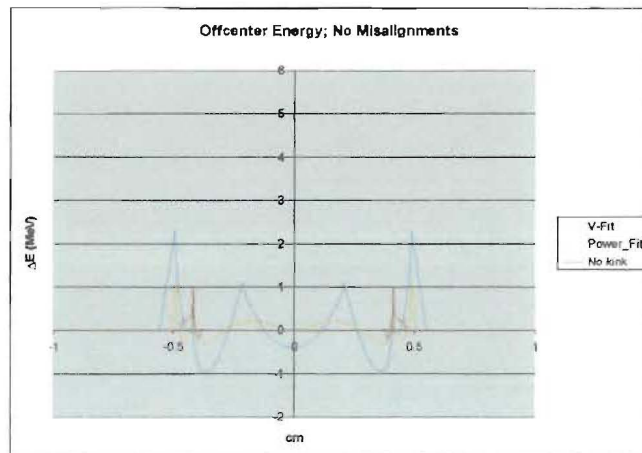
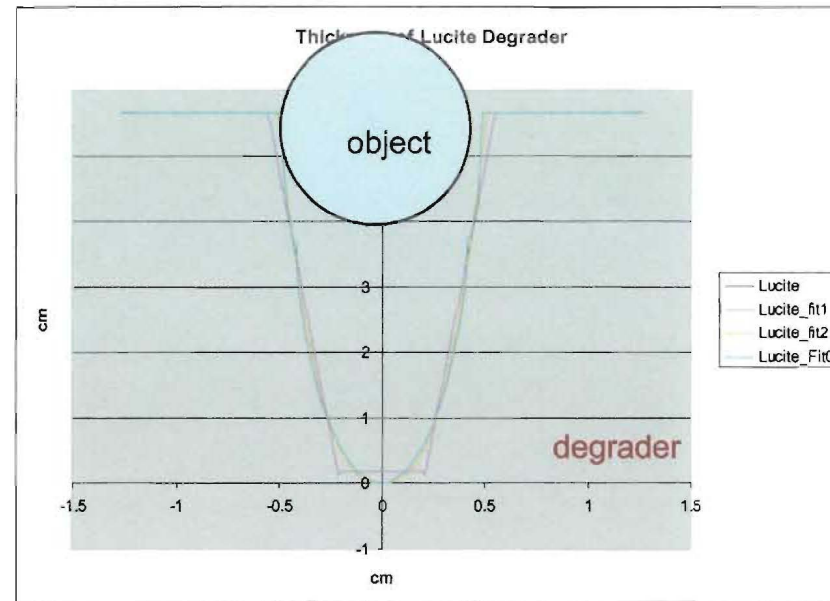
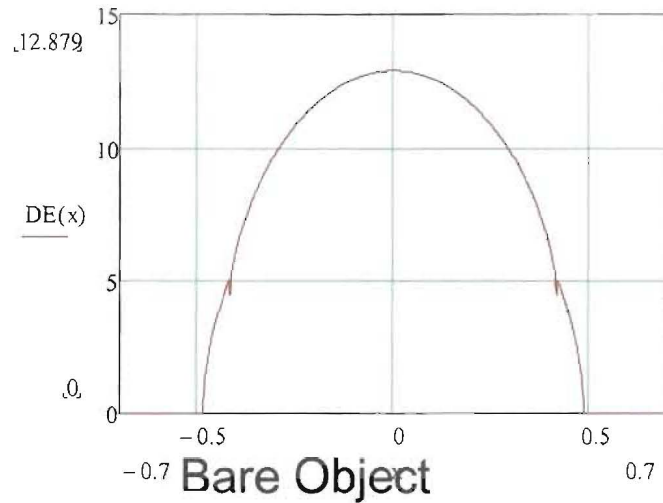
X3 magnifier has T126 ~ 3 meters

E-Loss through object center ~ 13 MeV → resolution ~ 0.5mm at center

Set the Lens to  $\langle E_{\text{Loss}} \rangle \sim 10\text{MeV}$  → resolution ~ 0.113 mm at center

For Static Objects One can reduce chromatic blur by use of “Graded Degraders”

# E-Loses and X3 Lens Resolution

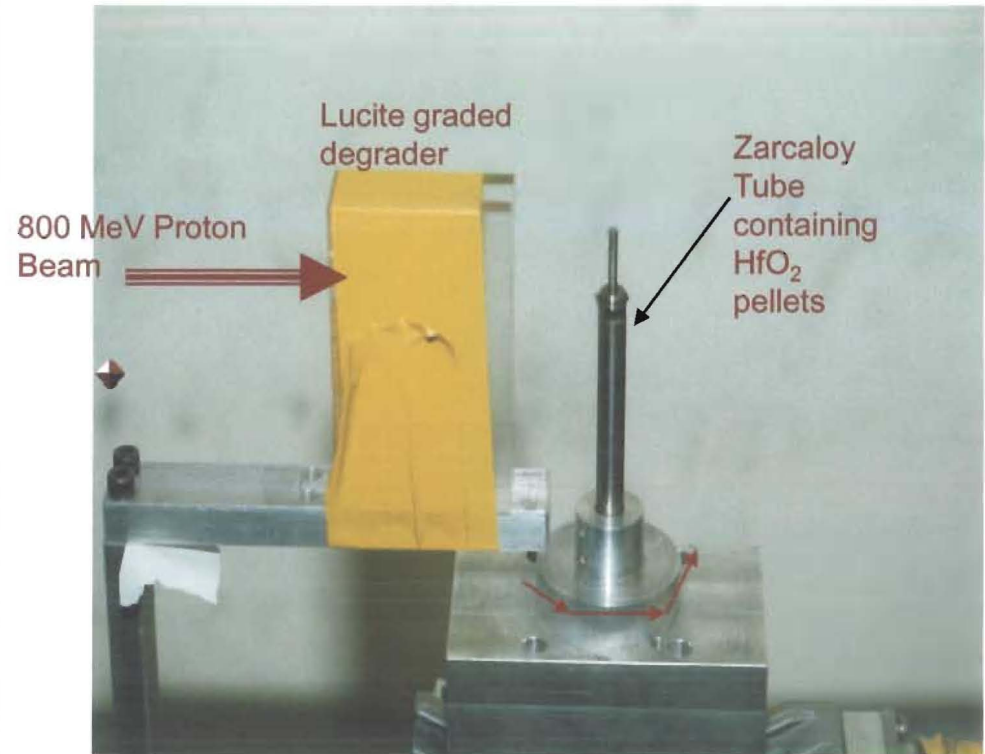
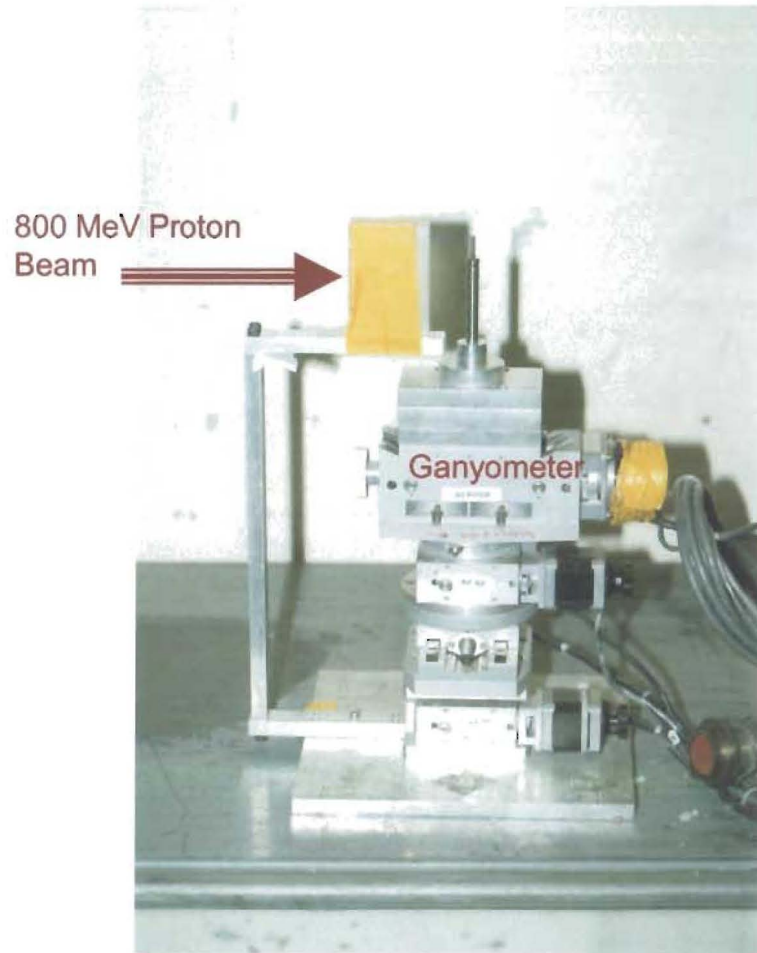


Object + Degrader

Intrinsic resolution  $\sim 65$  mm

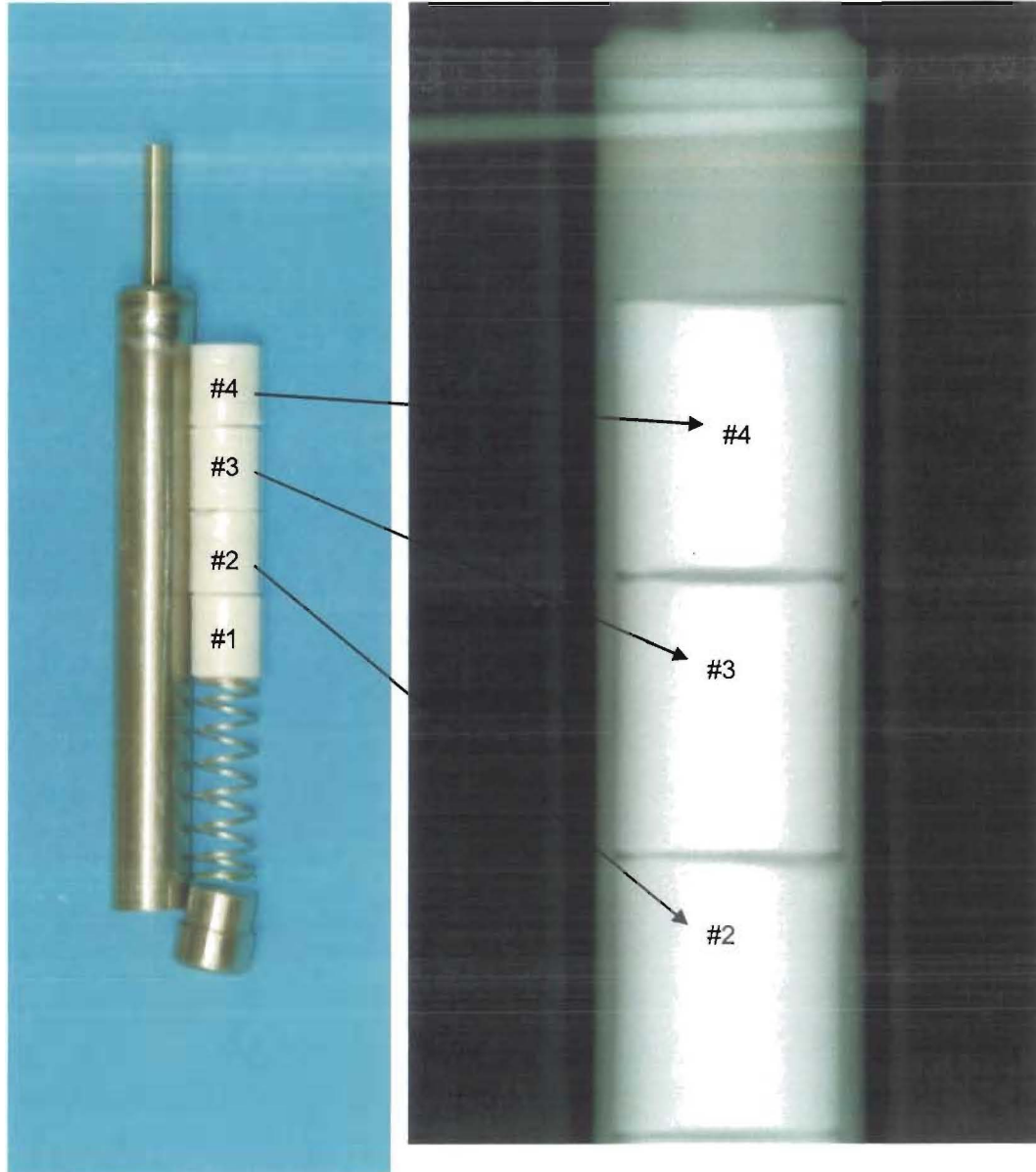
Chromatic term (T126) =  $3m \cdot \delta\theta \cdot (dE/E)$

# The Set up



Zircaloy tube was aligned on the graded degrader.  
Radiograph pictures were taken at 181 rotational positions

# Areal Density



# Relative Density Reconstruction



0°

45°

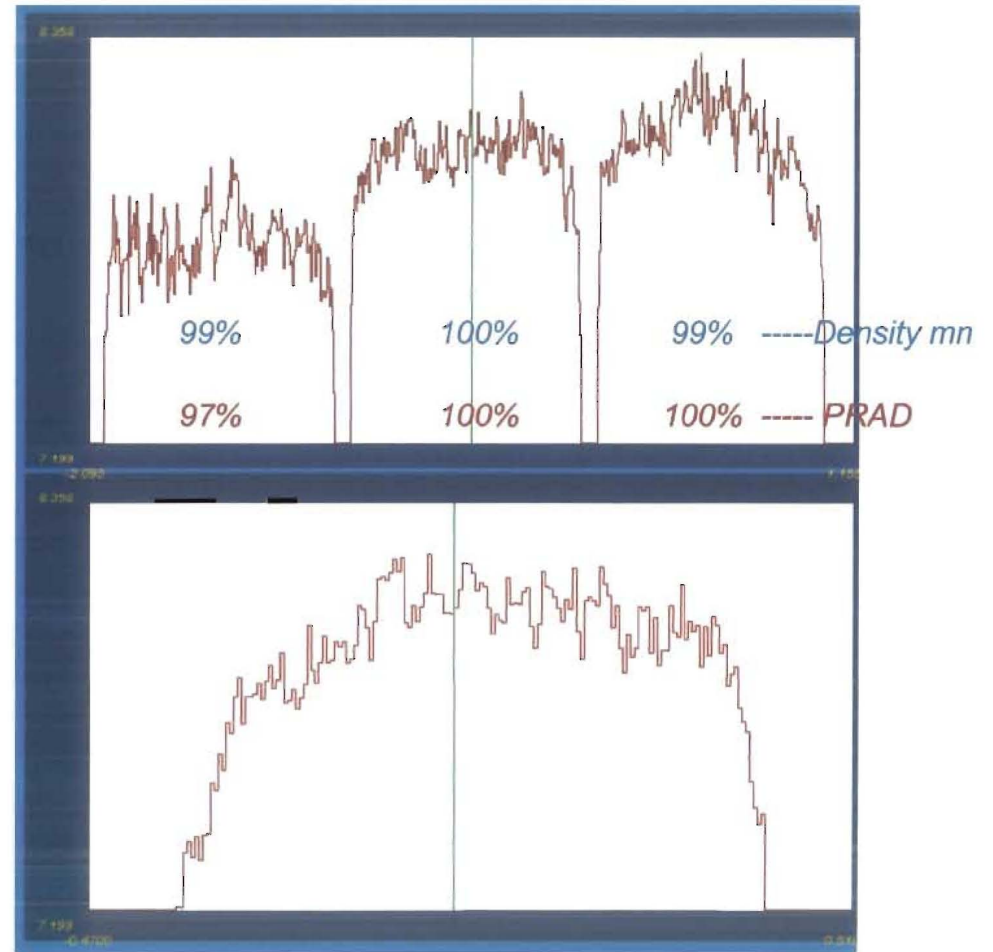
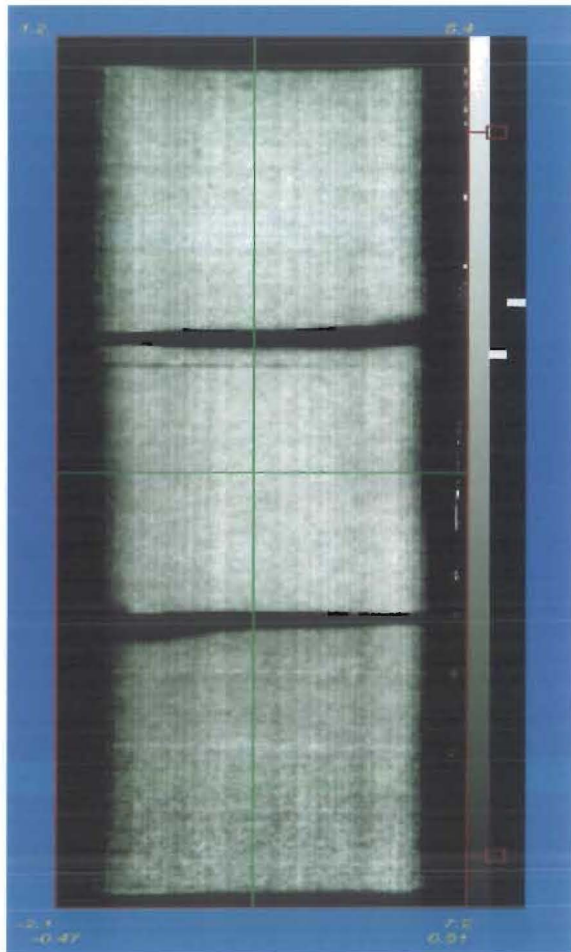
90°

135°

180°

Density reconstruction: Density measurements at

# Lineouts thru density reconstruction

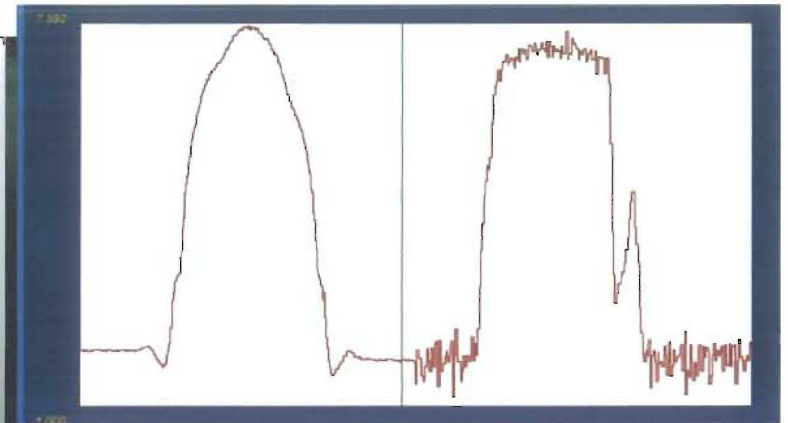
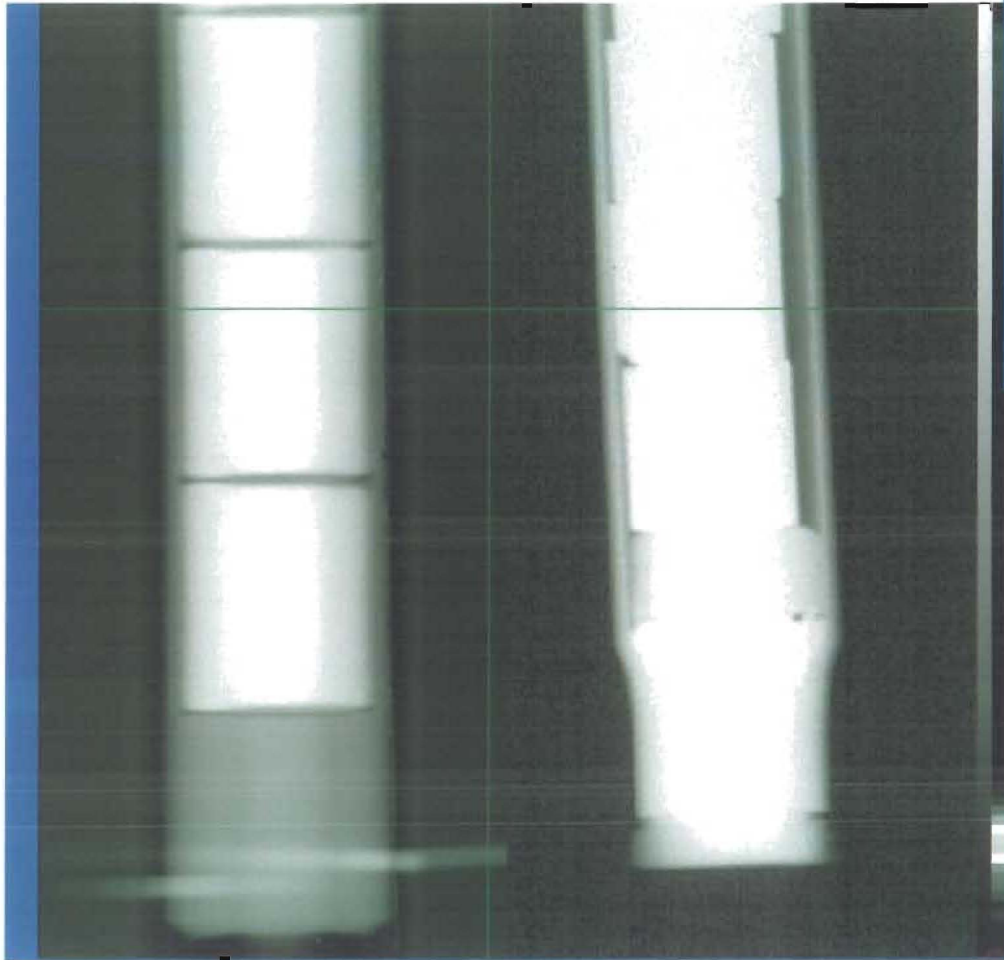


From fluctuations at flat top, measurement error ~1%

# pRad vs X-Ray radiographs

Protons

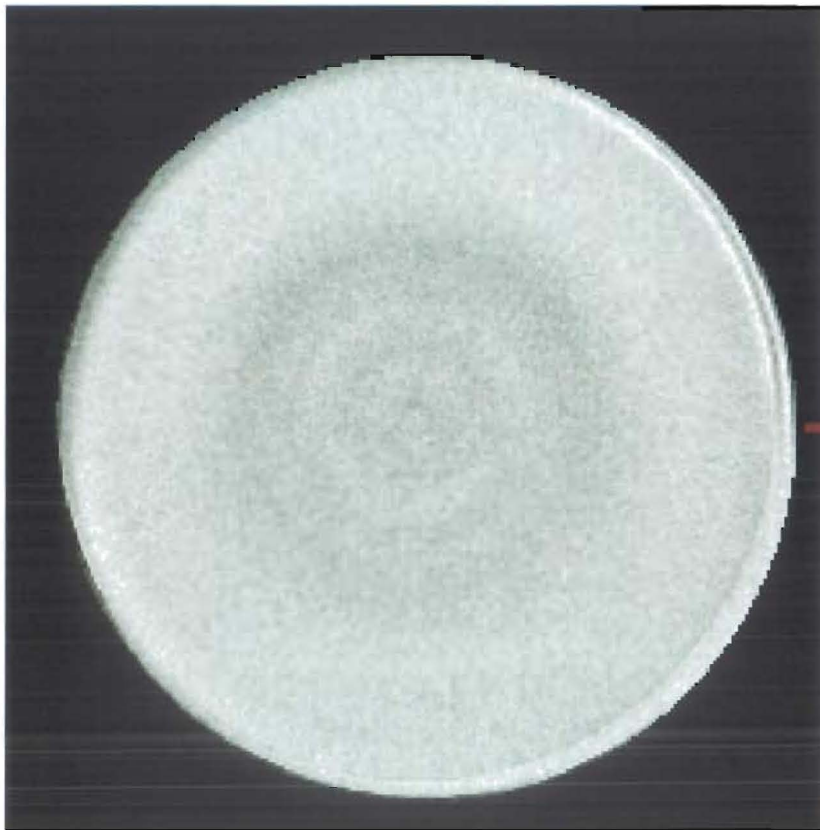
X-rays



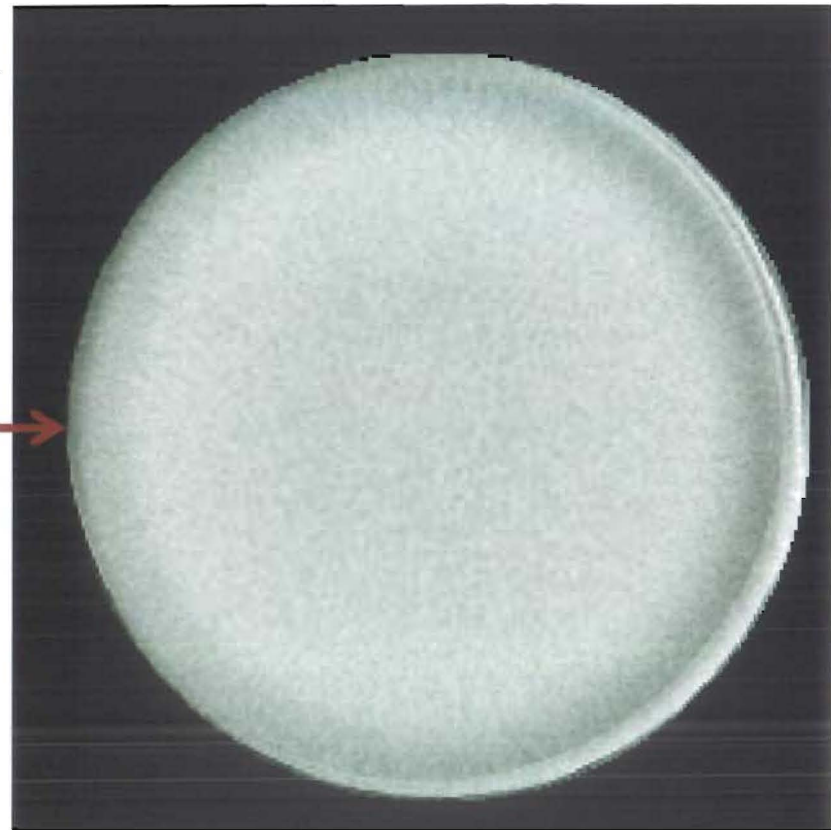
- Proton provide quantitative thickness information
- These X-ray images → don't penetrate and are dominated by scatter background
- Proton resolution can be improved with small angle collimator.
- X-rays need higher energy

CT Reconstruction: Minimize ring artifacts by assuming that the zarcaloy portion of the images is homogeneous and therefore has no ring structure in the density

**Default ring removal parameter**

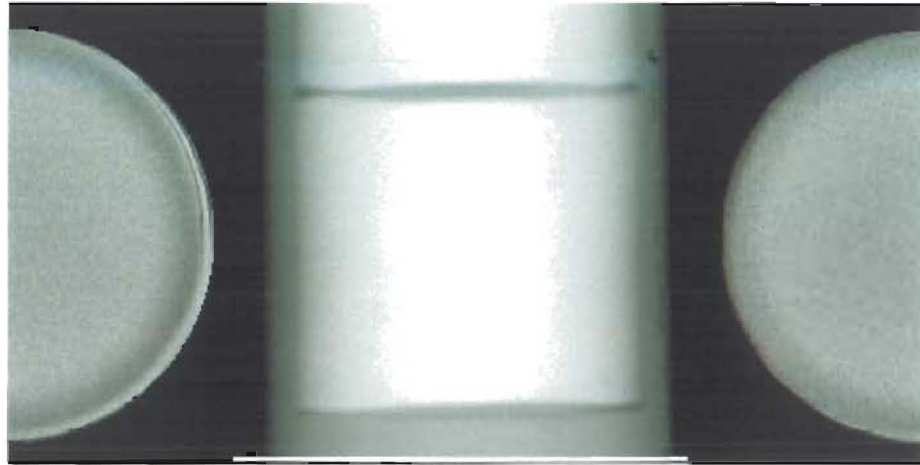


**Increased ring removal parameter**

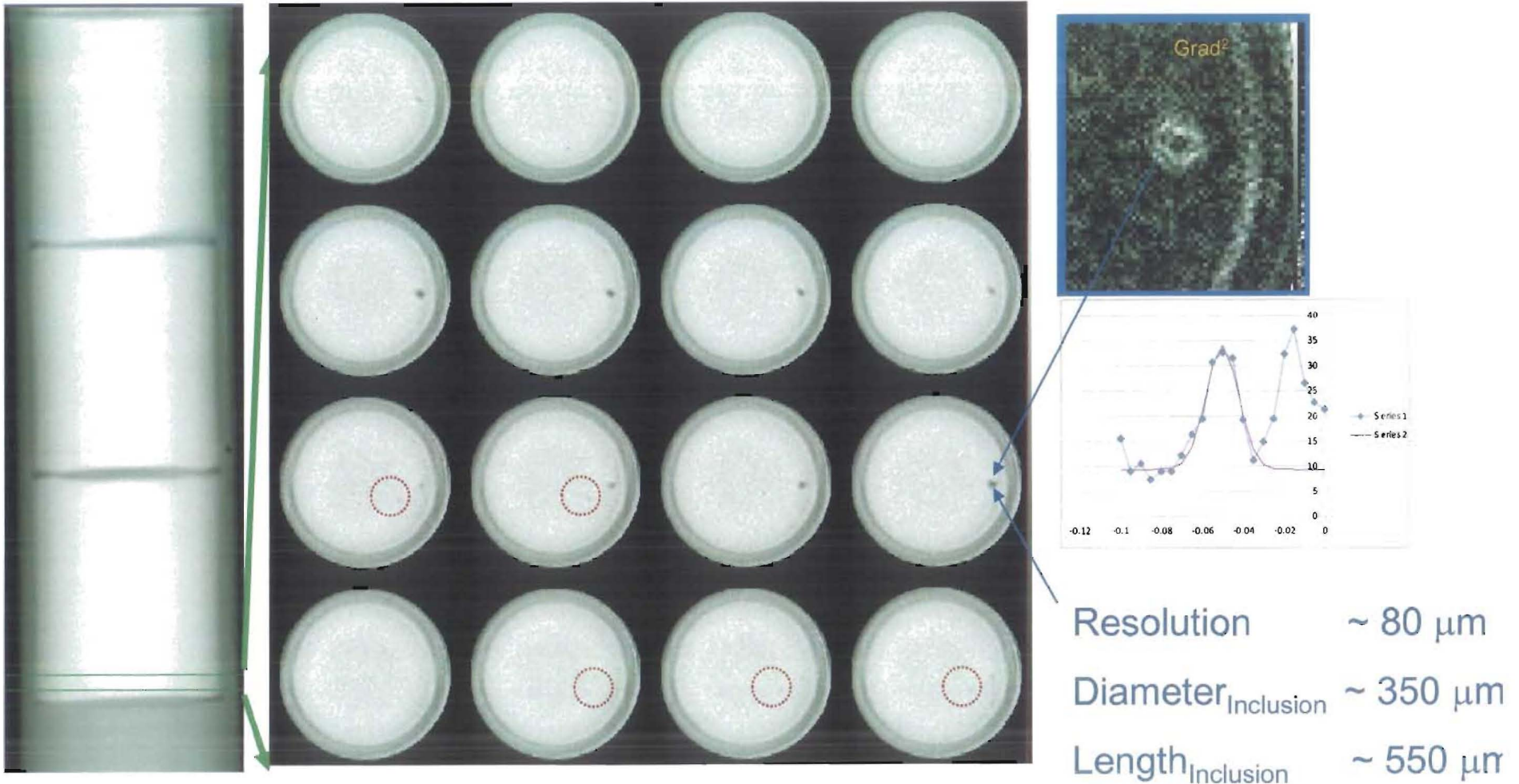


# CT Reconstructed Slices:

Interesting Regions: Part of Zircaloy portion, all of Pellet#4, Part of Pellet#3

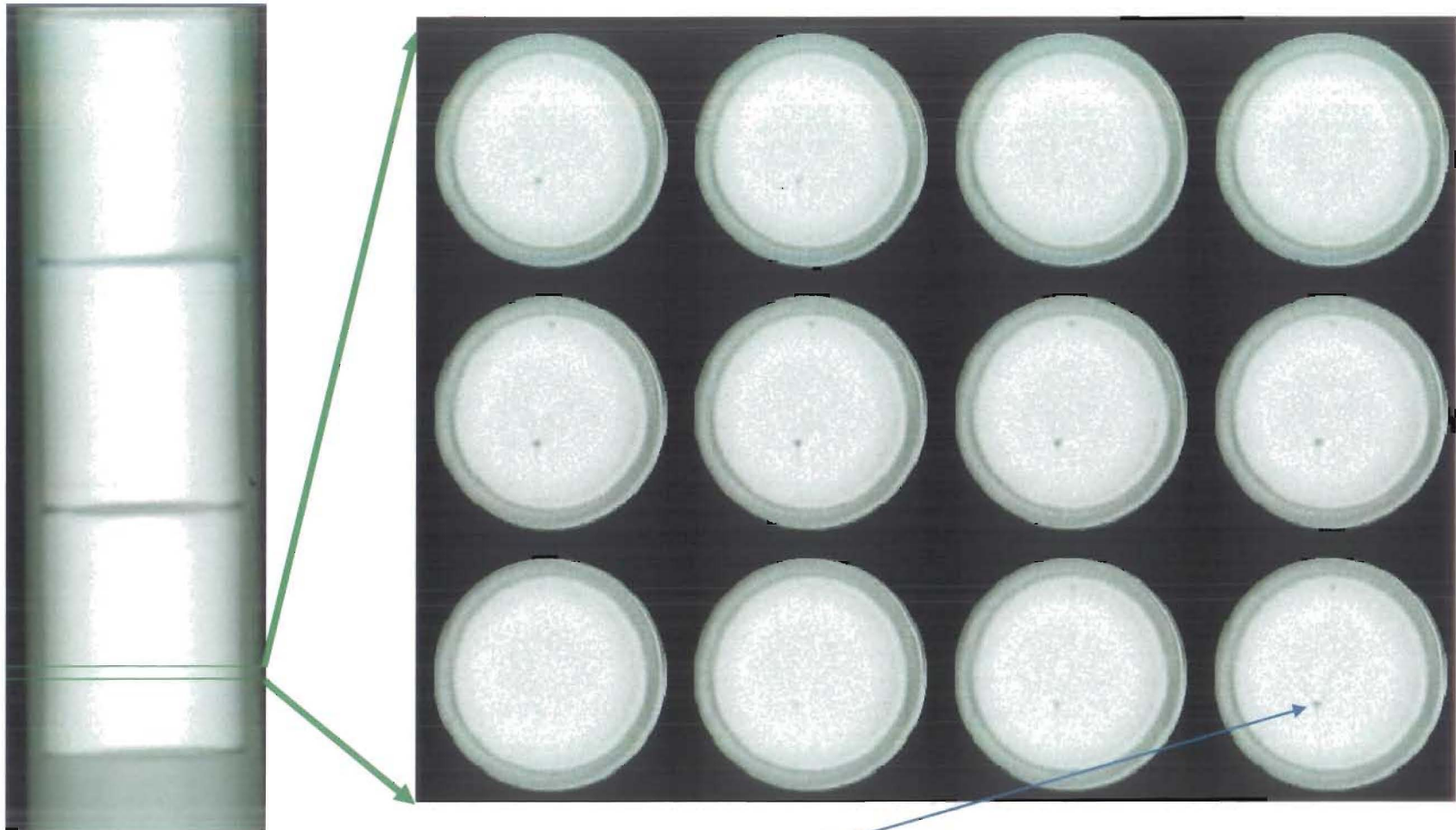


# Filtered Back Projection: Defects in Pellet #4, Slices 78 to 93



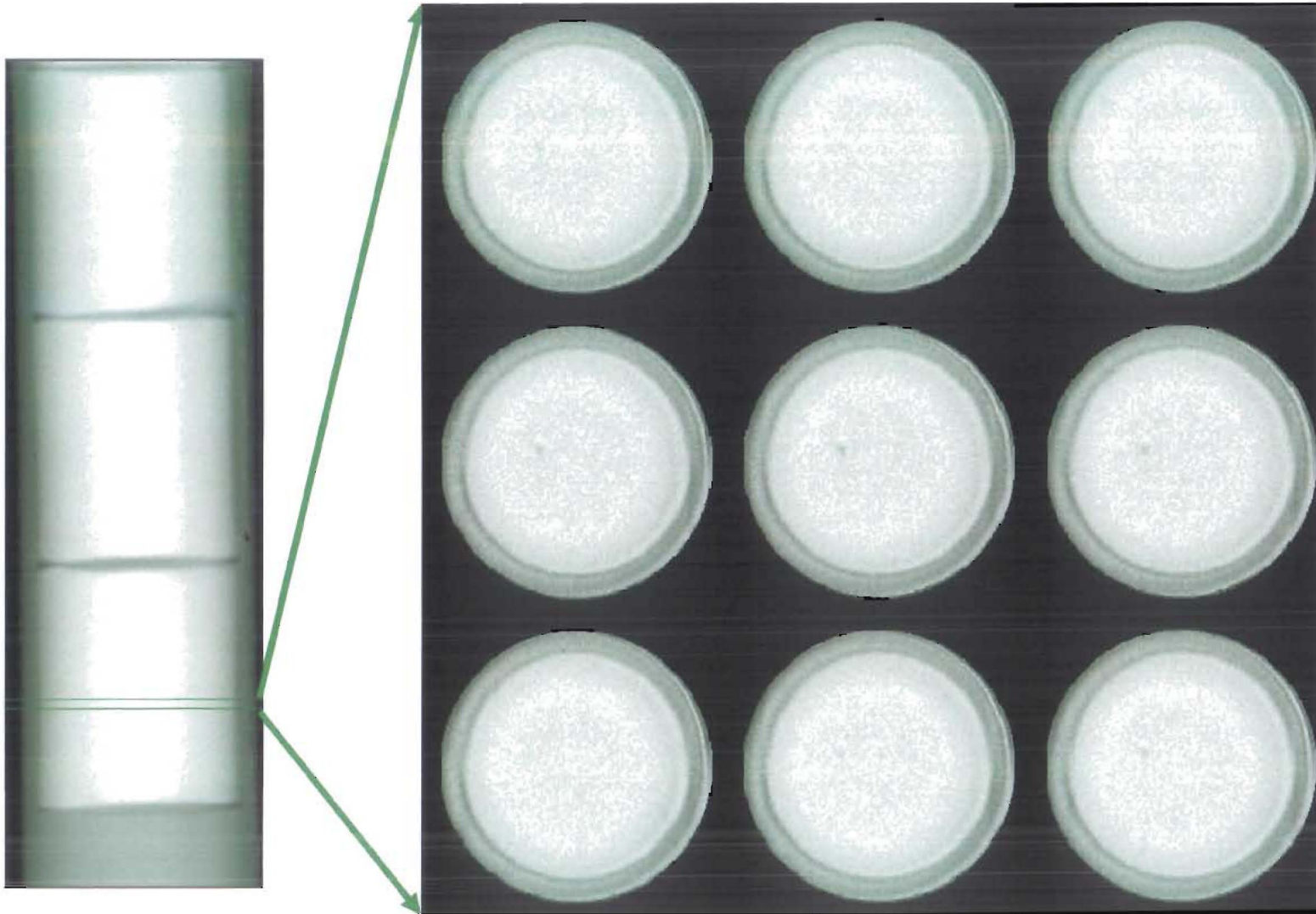
Fainter  $250 \mu\text{m}$  long by  $\sim 150$  to  $200 \mu\text{m}$  diameter inclusions are shown in the  circles

# More Defects in Pellet #4: Slices 131 to 142



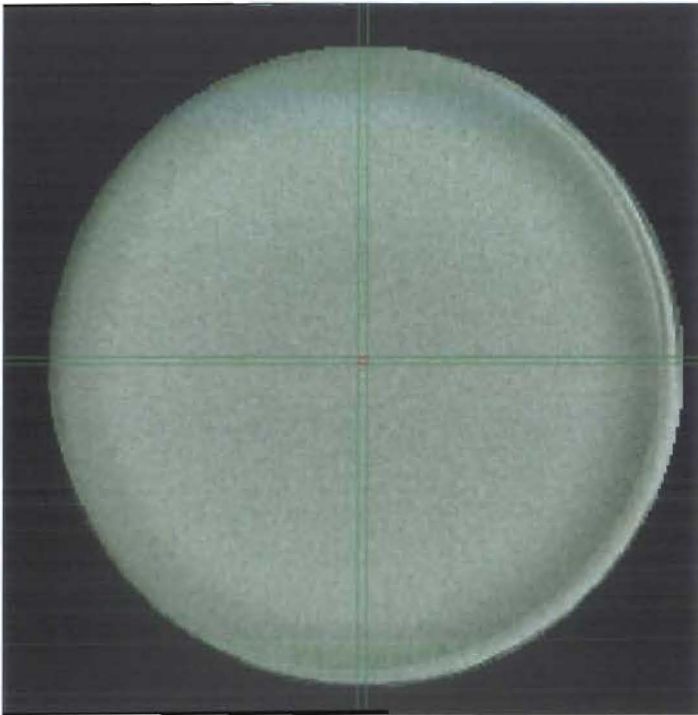
Diameter<sub>Inclusion</sub> ~ 225 μm  
Length<sub>Inclusion</sub> ~ 450 μm

# More Defects in Pellet #4: Slices 152 to 160

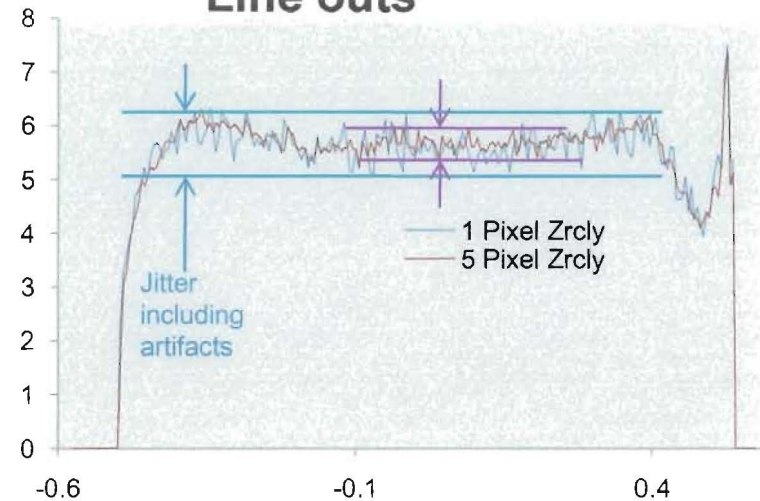


# Density reconstruction uncertainties from reconstructed Slices;

## A slice thru the zircaloy section



## Line outs



Single Pixel rms Jitter ~ 5%

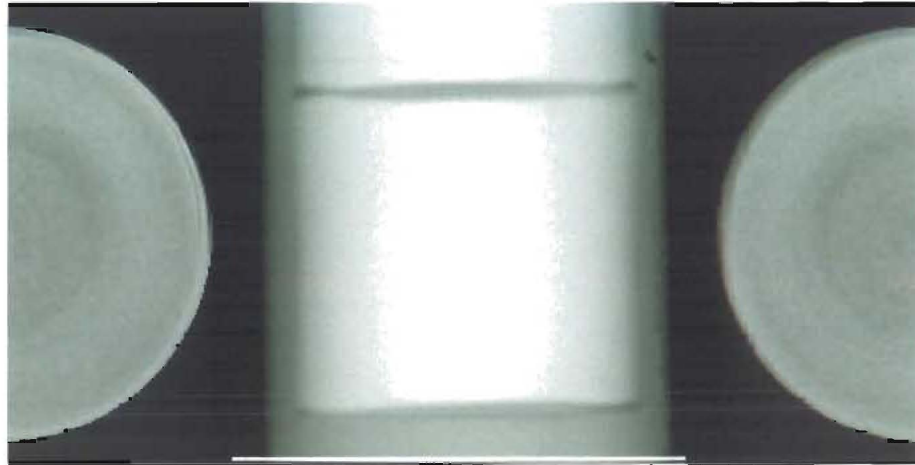
~4% no artifacts

Five Pixel rms Jitter ~3.5%

~2% no artifacts

Bad pixels due to tile boundary contribute to reconstruction artifacts above  
This can be avoided in future measurements  
Better CT algorithms can be used

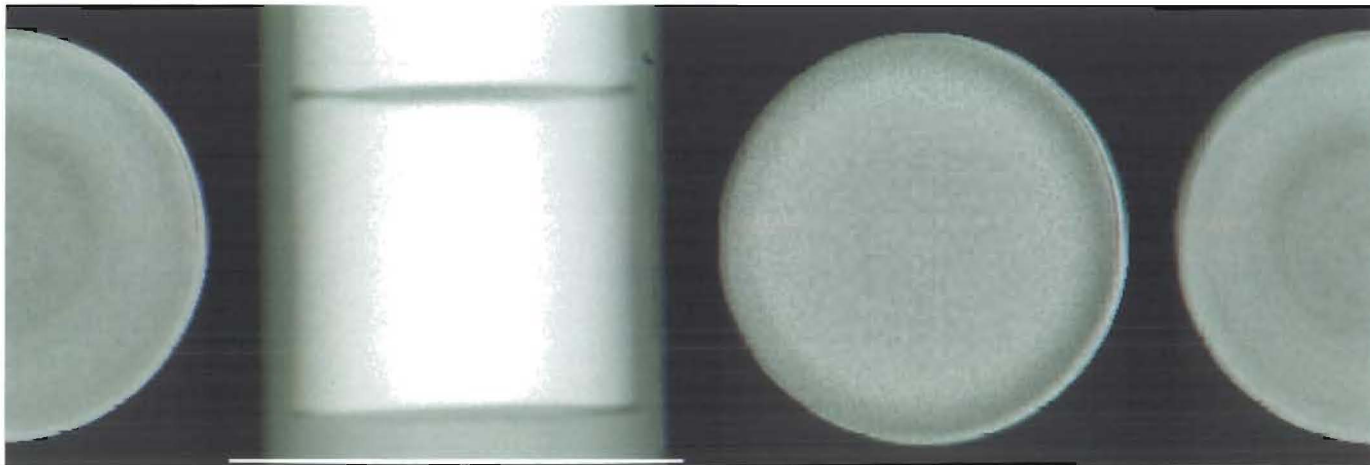
# Peter Smith's Reconstruction



# Comparison of two Independent CT Reconstructions

**FGM**

**Peter Smith**



# Summary: Imaging Lenses at pRad

*Includes lens and scintillator and camera lens*

LENSES SYSTEMS	Magnification	FOV	T126 (m) (Normalized)	T346 (m) (Normalized)	Bare Resolution (mm)	
LENS1 <i>7.5"</i>	-1	~120mm	6.9	6.9	<del>160</del> 160 $\mu$ m	
LENS2 <i>12"</i>	-1	120mm	7.9	7.9	180 $\mu$ m	
LENS3 <i>12"</i>	-1	120mm	7.9	7.9	180	
LENS2 & 3 <i>12"</i>	+1	120mm	15.8	15.8	280	
X3 <i>(4")</i> Magnifier	-3 <i>2.74</i>	40mm	4.4	3.89	6.5	
X7 <i>(1")</i> magnifier	-7	17mm	1.2	1.9	<i>~310</i> <i>(210 with image plates)</i>	<i>Needs to be commissioned</i>

# Concluding Remarks

- HE detonation characteristics are studied
- Material strength and EOS studies with HE or powder gun drivers
- Flexible timing possible due to versatility of the LANSCE proton beams
- Multiframe capability: up to 41 frames per dynamic event
- Rockwell cameras:
  - a) Acquire images over a wide range of frame rates (>0 to 30 Hz in movie mode and up to 4 MHz in standard triggering mode  
Facilitate easy acquisition of tomographic images
  - b) High QE → Equivalent to increasing beam by factor of 4
- x 3 and x7 magnifier, with reduced chromatic blur useful to enhances resolution and reducing chromatic blur – good for radiographing small objects